Bifurcation of sharp boundary =1 multipole equilibria

Ross L. Spencer

Citation: Physics of Fluids (1958-1988) **23**, 1691 (1980); doi: 10.1063/1.863188
View online: http://dx.doi.org/10.1063/1.863188
View Table of Contents: http://scitation.aip.org/content/aip/journal/pof1/23/8?ver=pdfcov
Published by the AIP Publishing

Bifurcation of sharp boundary $\beta=1$ multipole equilibria

Ross L. Spencer[a)]

Department of Physics, University of Wisconsin–Madison, Madison, Wisconsin 53706
(Received 11 October 1979; accepted 9 May 1980)

The bifurcation of sharp boundary magnetohydrodynamic equilibria in linear multipoles of arbitrary order is studied using the hodograph method. In the low pressure limit, simple formulae are obtained for the shapes of multipole cusp equilibria. In the high pressure limit the equilibria are found to bifurcate; two different equilibria may exist for the same values of the external parameters. It is conjectured that a similar bifurcation will be encountered in the calculation of diffuse multipole equilibria at high beta.

I. INTRODUCTION

The multipole geometry for thermonuclear plasma confinement has received renewed interest in the last few years because of its suitability for use with advanced fuels.[1,2] This renewed interest has consisted, in part, of theoretical efforts to understand the equilibrium and stability at high beta of such devices.[3,4] A way of studying equilibrium at high beta that has been used extensively in the study of tokamaks is to assume that the plasma is confined only by surface currents that act to exclude the magnetic field from the plasma; that is, the equilibrium is assumed to be a $\beta=1$ sharp boundary equilibrium. An advantage of such a formulation of the equilibrium problem is that when it is applied in a linear geometry, i.e., in a geometry with two Cartesian dimensions, the hodograph method of fluid mechanics can be applied.[5,6] The use of this method for solving magnetohydrodynamic equilibrium problems extends from the early work of Berkowitz *et al.*[7,8] on cusp equilibria, through several sharp boundary tokamak-related studies,[9-11] some of which use variations of the usual hodograph method,[12-16] to the work of Fried *et al.*[17] on surface magnetic field configurations and that of Shercliff[18] on cusp and divertor equilibria. Here, an extension of the cusp work of Berkowitz *et al.* and Shercliff to sharp boundary equilibria of nth-order linear multipoles without conducting walls is presented.

Cusp equilibria of the kind shown in Fig. 1 and closed equilibria of the kind shown in Fig. 2 are studied. In order to determine a closed equilibrium, the multipole order n, the fluid pressure, the wire currents and positions, and a quantity χ related to the total axial current flowing on the fluid surface must be specified. It is found that closed equilibria, if they exist at all, exist for values of the pressure in an interval whose endpoints are determined by the other four parameters. This interval never includes zero pressure. At low pressures it is found that the same parameters also uniquely determine a multipole cusp equilibrium, but as the pressure is increased, holding the other parameters fixed, the situation becomes more complicated. Sometimes there are closed and cusp equilibria with the same parameter values, and sometimes there are two cusp equilibria with the same parameter values. Thus, in the transition between cusp and closed equilibria, bifurcation is encountered. These high pressure cusp equilibria and the closed equilibria all have regions of bad curvature on their boundaries and are hence unstable.[19] An understanding of these equilibria and the nature of their bifurcation is the object of this paper.

II. CLOSED EQUILIBRIA

Here, closed equilibria like the one shown in Fig. 1 are discussed. Consider n infinitely long straight wires, equally spaced around a circle of radius a, and each carrying a current I. The wires and the vacuum regions associated with them are imbedded in a simple sharp boundary z-pinch equilibrium of circular cross section. Such an equilibrium is completely characterized by specifying n, I, a, the fluid pressure p, and a quantity χ defined by

$$\chi = I_f/nI\,, \tag{1}$$

where I_f is the total axial current flowing on the fluid surface. It is convenient to define a quantity b by

$$b=(2\mu_0 p)^{1/2}\,. \tag{2}$$

Since the equilibrium has a sharp boundary with no magnetic field inside, b is the magnetic field strength at the vacuum-fluid interface. Pressure balance and the expression for the magnetic field of a current carrying cylinder are used to obtain r_1, the radius of the vacuum region about each wire, and r_2, the radius of the outer fluid surface:

$$r_1 = \mu_0 I/2\pi b\,, \tag{3}$$

$$r_2 = n(\chi+1)r_1\,. \tag{4}$$

Equilibria of this type do not exist for arbitrary choices of the determining parameters. They exist if, and only if, (i) the outer fluid boundary does not intersect an inner fluid boundary, i.e.,

$$r_2 > r_1 + a\,, \tag{5}$$

and (ii) two inner fluid boundaries do not intersect, i.e.,

$$r_1 < a\sin(\pi/n)\,. \tag{6}$$

The inequalities (5) and (6) can be arranged to give a necessary and sufficient condition for the existence of a closed equilibrium

$$[\sin(\pi/n)]^{-1} < \gamma < [n(\chi+1)-1]\,, \tag{7}$$

---

a)Present address: Los Alamos Scientific Laboratory, University of California, Los Alamos, N. M. 87545.

 0031-9171/80/081691-07$00.90

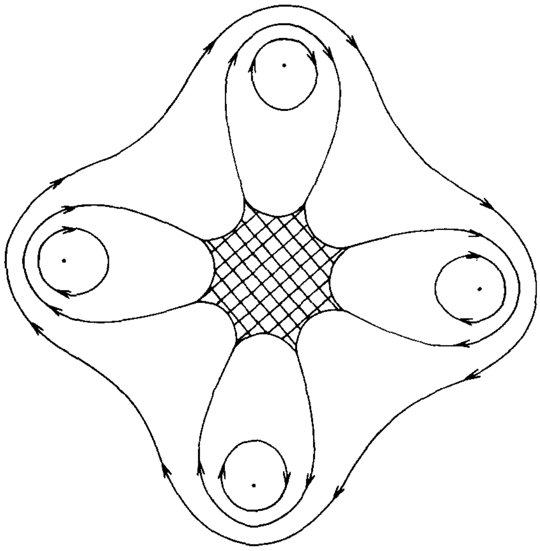

FIG. 1. The free boundary and some field lines of a sharp boundary $\beta = 1$ octupole cusp equilibrium are shown. The conducting fluid is indicated by the cross hatching.

where

$$\gamma = 2\pi ab/\mu_0 I . \tag{8}$$

This condition cannot be satisfied for any value of γ if χ is too small; closed equilibria exist only if

$$\chi > \frac{1}{n}\left(\frac{1}{\sin(\pi/n)} + 1\right) - 1 . \tag{9}$$

For the case of an octupole ($n = 4$), χ must be greater than -0.396. Note that the flux between the wire and the inner fluid surface, although infinite, is proportional to I. Hence, keeping I fixed corresponds to conservation of this infinite flux. Similarly, outside the fluid column, flux conservation corresponds to fixed I_f, or equivalently, fixed χ.

The more complicated cusp equilibria and their transition to the closed equilibria discussed here are now considered.

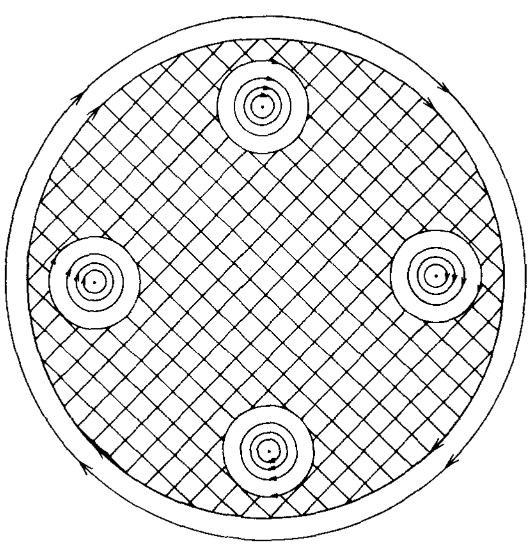

FIG. 2. The free boundary and some field lines of a sharp boundary $\beta = 1$ octupole closed equilibrium are shown. The conducting fluid is indicated by the cross hatching.

III. CUSP EQUILIBRIA

A. The hodograph method

In order to find the cusp equilibria, a conformal mapping technique invented by Helmholtz[5] is used. Consider the sector of the x-y plane shown in Fig. 3. By symmetry, such a sector is the only portion of the plane that need be studied. The letters A–F are used to refer to important points in the sector. The two Cartesian coordinates, x and y, are combined to form one complex variable

$$z = x + iy . \tag{10}$$

The magnetic field components, B_x and B_y, are combined to form a complex magnetic field variable

$$w = B_x - iB_y . \tag{11}$$

A complex magnetic potential is defined by

$$F = \phi + i\psi , \tag{12}$$

where ϕ is the real magnetic potential, i.e.,

$$\mathbf{B} = \nabla\phi , \tag{13}$$

and where ψ is the flux function related to B by

$$B_x = \frac{\partial\psi}{\partial y} , \quad B_y = -\frac{\partial\psi}{\partial x} . \tag{14}$$

These three complex quantities are related by

$$\frac{dF}{dz} = w . \tag{15}$$

Since the equilibrium is assumed to be a sharp boundary equilibrium with no field in the fluid, the only magnetic field in the problem is the vacuum field. Since B_x and B_y, in vacuum, each satisfy Laplace's equation, any analytic function $w(z)$ automatically describes a vacuum magnetic field; the function $w(z)$ that solves the problem is determined by the boundary conditions. The boundary conditions are that ψ is constant on any conducting surface, that near a wire, or far away from the currents, the magnetic field is that of an infinitely long straight wire carrying the appropriate

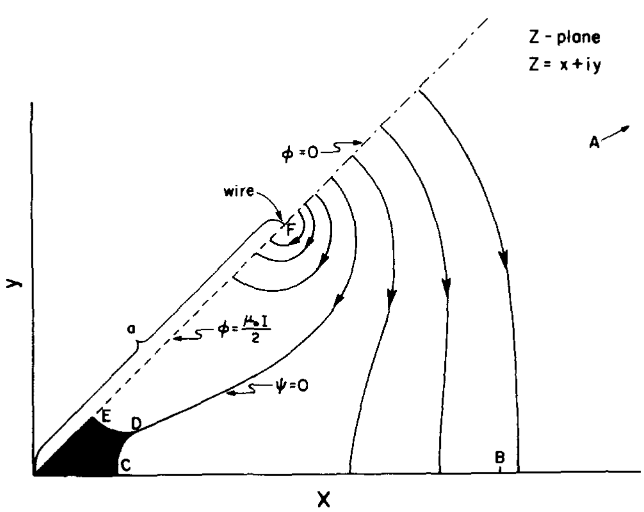

FIG. 3. A sector of the z plane for a low pressure octupole cusp equilibrium with $\chi = 0$ is shown.

current, and that at the surface of the free boundary

$$|\mathbf{B}| = (2\mu_0 p)^{1/2} . \tag{16}$$

This would be a simple boundary value problem except that the position of the fluid boundary is unknown. Hence, the usual technique of conformally mapping the F plane to the z plane cannot be applied. Helmholtz's technique relies instead on Eq. (15). Using analysis and physical intuition, the images of the z plane sector in the complex F and w planes are constructed. The F and w plane images are mapped conformally to each other to give $w(F)$, and Eq. (15) is then integrated to obtain $F(z)$, solving the problem.

B. General solution

In order to determine a cusp equilibrium, it is necessary, as in Sec. II, to specify n, I, a, p (or b), and χ. For a cusp equilibrium, the definition of χ is

$$\chi = 2(I_{\mathrm{DE}} - I_{\mathrm{CD}})/I , \tag{17}$$

where I_{DE} is the total axial current flowing in the free boundary between points D and E in Fig. 3, and where I_{CD} is that flowing between points C and D. Note that the current in adjacent free boundary segments flows in opposite directions. Here, as in Sec. II, I held constant corresponds to flux conservation between the wire and the fluid, and χ held constant corresponds to flux conservation between the fluid and infinity. Figure 3 illustrates a sector of an octupole cusp with $\chi = 0$.

The problem is solved by mapping both the F plane, shown in Fig. 4, and the w plane, shown in Fig. 5, to the intermediate λ plane, shown in Fig. 6. The functions that affect these mappings are

$$F(\lambda) = \frac{\mu_0 I}{2}\left[\frac{i}{\pi}(\chi+1)\cosh^{-1}\lambda + \frac{i}{\pi}\ln\left(\frac{(\lambda^2-1)^{1/2}+(r^2-1)^{1/2}}{\lambda+r} - \frac{r}{(r^2-1)^{1/2}}\right) + \chi + 2 + \frac{i}{2\pi}\ln(r^2-1)\right], \tag{18}$$

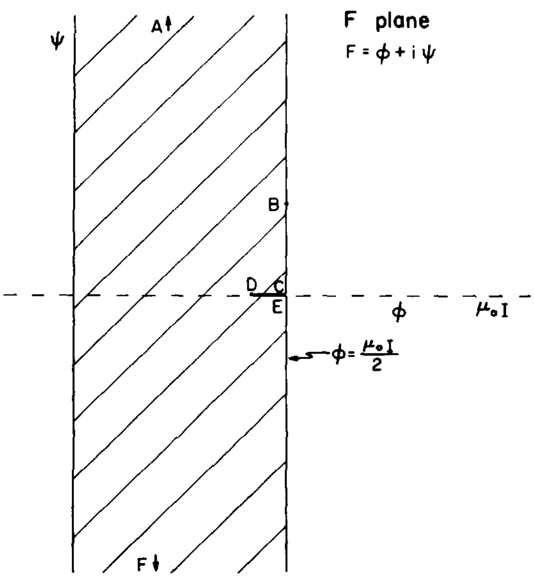

FIG. 4. The F-plane image of the z-plane sector of Fig. 3 is shown.

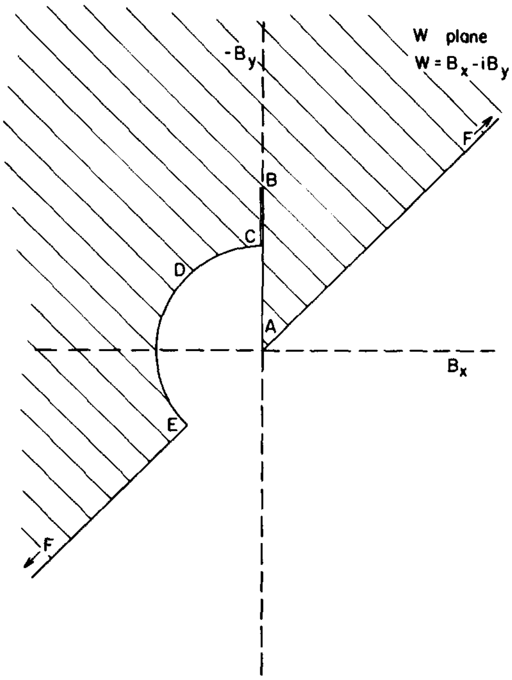

FIG. 5. The w-plane image of the z-plane sector of Fig. 3 is shown.

$$w(\lambda) = -ib\left[(r^2-1)^{1/2}[\lambda+(\lambda^2-1)^{1/2}]^{1/n} \times\left(\frac{(\lambda^2-1)^{1/2}+(r^2-1)^{1/2}}{\lambda+r} - \frac{r}{(r^2-1)^{1/2}}\right)\right]^{-1}, \tag{19}$$

where b is defined in Eq. (2). The quantity r is associated with the λ plane image of the point F. The quantities t and s, associated with points B and D in the λ plane, are given in terms of χ and r by

$$s = (r^2-1)^{1/2}/(\chi+1) - r , \tag{20}$$

$$t = n(r^2-1)^{1/2} - r . \tag{21}$$

Large r corresponds to low pressure cusp equilibria, while as r approaches 1, a smooth transition is made to closed equilibria. Note that as r approaches 1, t becomes less than 1, i.e., point B crosses point C on the

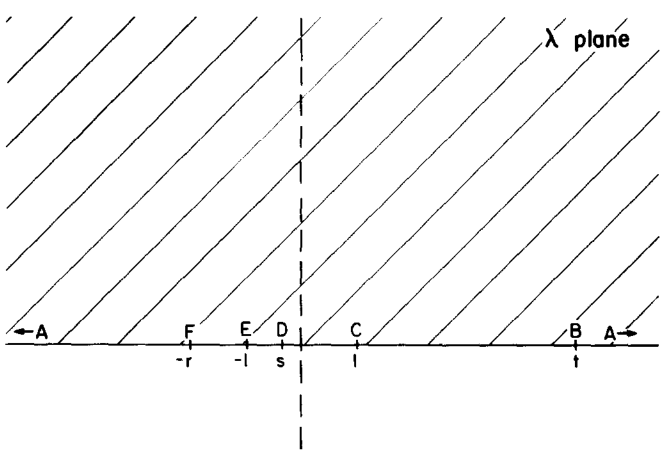

FIG. 6. The λ-plane image of the z-plane sector of Fig. 3 is shown.

fluid boundary. When this happens, point B ceases to be a point of maximum field magnitude on the ray CA in Fig. 3, and instead becomes a point of inflection on the free boundary; the boundary segment CB then curves outward, while the segment BD has the inward curvature required in the neighborhood of the cusp point, D. The appearance of outward curvature makes the equilibrium unstable to flute modes localized in the region of outward curvature.[19] Thus, $t=1$ marks the transition from stable to unstable equilibria.

The solution is completed by determining the quantity r in terms of the physical parameters. This is done by requiring that the wire be at the position $z=a[\exp(i\pi/n)]$ in Fig. 3. Making the change of variable

$$\lambda=\cosh(\eta) \tag{22}$$

and using Eqs. (15), (18), and (19) yields a differential equation for $z(\eta)$:

$$\frac{dz}{d\eta}=\frac{\mu_0 I(\chi+1)}{2\pi b}\,\frac{\exp(\eta/n)(\cosh\eta-s)}{\cosh(\eta+\eta_0)+1}, \tag{23}$$

where

$$\cosh\eta_0=r. \tag{24}$$

(Note that η and λ are complex variables; care must be taken to properly analytically continue expressions containing them.) Requiring the wire to be at the proper position relates r and γ, defined in Eq. (8), by

$$\gamma=h(r)\equiv l(r)+\frac{j(r)}{\sin(\pi/n)}, \tag{25}$$

where

$$l(r)=(\chi+1)\int_0^{\eta_0}\frac{\exp(\xi/n)(\cosh\xi+s)}{\cosh(\xi+\eta_0)-1}\,d\xi, \tag{26}$$

and where

$$j(r)=\mathrm{Re}\left((\chi+1)\int_0^{\pi}\frac{\exp(i\theta/n)(\cos\theta-s)}{\cosh(i\theta+\eta_0)+1}\,d\theta\right). \tag{27}$$

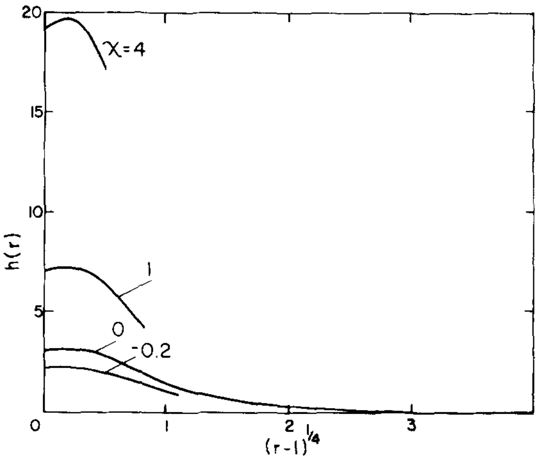

FIG. 7. The function h is displayed vs $(r-1)^{1/4}$ for $\chi=4$, 1, 0, and -0.2, and for $n=4$, an octopole. The $\chi=4$, 1, and -0.2 curves stop when the equilibria neck off.

The function $h(r)$ is shown in Fig. 7 for several values of χ. Note that for r near 1 and for χ such that closed equilibria exist, there are two equilibria for each value of γ, either a closed equilibrium and a cusp equilibrium, or two cusp equilibria. If we imagine performing a thought experiment in which n, I, a, and χ are held fixed as the pressure is lowered from some high value, no equilibria will be obtained at first; when the pressure reaches a critical value, one cusp equilibrium will be obtained, and further decreases in the pressure will allow two cusp equilibria to exist. One of the cusp equilibria will evolve into a closed equilibrium, while the other will remain cusp-like as the pressure is decreased further.

Detailed information about the equilibria can be obtained by integrating Eq. (23). For a given value of n it appears to be possible to integrate Eq. (23) in closed form; for an octupole the result is

$$\frac{z}{a}=(\chi+1)\frac{2}{[r+(r^2-1)^{1/2}]^{1/4}}\left[\frac{2[\lambda+(\lambda^2-1)^{1/4}]}{[r+(r^2-1)^{1/2}]^{3/4}}+(r^2-1)^{1/2}\left(2-\frac{1}{2(\chi+1)}\right)\left(\coth^{-1}\{[r+(r^2-1)^{1/2}][\lambda+(\lambda^2-1)^{1/2}]\}^{1/4}\right)\right.$$
$$\left.+\tan^{-1}\{[r+(r^2-1)^{1/2}][\lambda+(\lambda^2-1)^{1/2}]\}^{1/4}\Big)-\frac{(r^2-1)^{1/2}}{(\chi+1)}\,\frac{[r+(r^2-1)^{1/2}]^{1/4}[\lambda+(\lambda^2-1)^{1/2}]^{1/4}}{[r+(r^2-1)^{1/2}][\lambda+(\lambda^2-1)^{1/2}]-1}\right]+\text{const}. \tag{28}$$

This rather formidable expression gives insight only in special limits, although it is very useful for numerically determining the free boundary shapes and the function $h(r)$. Figures 8–11, showing some free boundary shapes, were obtained using Eq. (28). Figures 8–10 show equilibria with χ fixed for various values of γ; Fig. 11 shows equilibria with γ fixed for various values of χ.

There is a special quantity that gives qualitative information about the free boundary. It is the quantity α defined by

$$\alpha=L_{DE}/L_{CD}, \tag{29}$$

where L_{DE} is the length of the free boundary segment DE while L_{CD} is that of the segment CD. The mapping function $F(\lambda)$ and Ampere's law are used to obtain

$$\alpha=1+\pi\chi\{\cos^{-1}[r-(\chi+1)(r^2-1)^{1/2}]-(\chi+1)\cos^{-1}[r-(r^2-1)^{1/2}/(\chi+1)]\}^{-1} \tag{30}$$

This relatively simple expression gives the elongation of one segment over its neighbor; note that if $\chi=0$, then $\alpha=1$, as expected. This quantity is especially useful for describing low pressure cusp equilibria.

C. The low pressure limit

If we imagine decreasing the fluid pressure, or γ, to lower and lower values holding n, I, a, and χ fixed, then unless $|\chi|\ll 1$, equilibria will cease to exist below some critical pressure. This occurs because the free

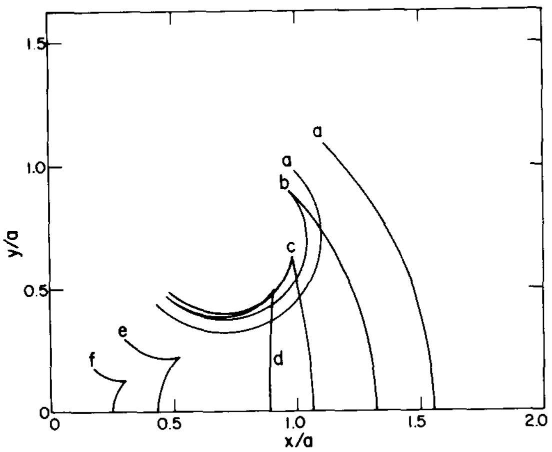

FIG. 8. Free boundary shapes for $\chi=0$ and $n=4$ are shown. (a) $\gamma=2.57$, (b) $\gamma=3.02$, (c) $\gamma=3.02$, (d) $\gamma=2.57$, (e) $\gamma=0.5$, and (f) $\gamma=0.1$.

boundary "necks off,"[18] i.e., two different segments of the boundary touch. To see why this happens, note that Ampere's law can be used to write χ in the form

$$\chi=(2b/\mu_0 I)(L_{DE}-L_{CD}). \tag{31}$$

Decreasing b thus requires $L_{DE}-L_{CD}$ to increase, unless χ is nearly zero. For closed equilibria, this eventually causes the circular surfaces around neighboring wires to intersect, causing loss of equilibrium. For cusp equilibria, a similar process occurs; one of the two segments must become much longer than the other, until neighboring segments touch, or "neck off," as illustrated in Figs. 9(d) and 10(d). This loss of cusp equilibrium for χ not near zero is the reason for the termination of the curves in Fig. 7. The study of low pressure equilibria is thus the study of equilibria with $\chi\simeq 0$.

From Fig. 7 it is clear that the low pressure limit is obtained by letting r become large. Expanding in $1/r$, and keeping only leading terms, the low pressure limit of $h(r)$ is

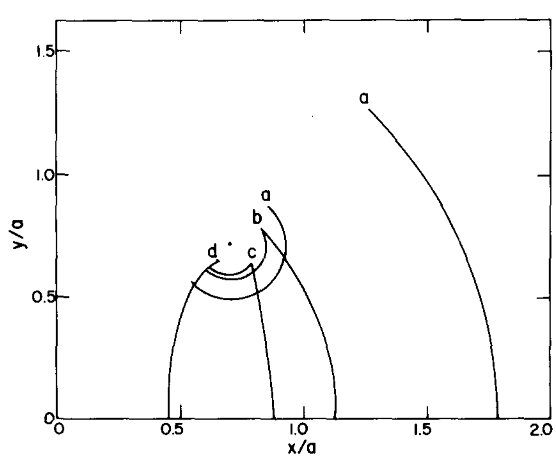

FIG. 9. Free boundary shapes for $\chi=1$ and $n=4$ are shown. (a) Closed equilibrium with $\gamma=4.53$, (b) $\gamma=7.05$, (c) $\gamma=7.05$, and (d) $\gamma=4.53$. [Note that (d) is a necked off equilibrium; it touches another segment on the line between the center and the wire.]

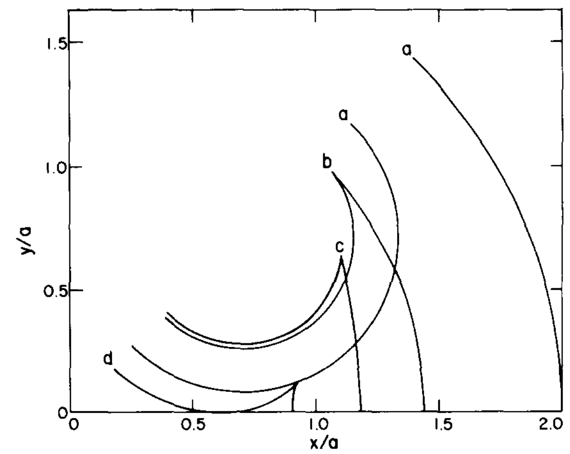

FIG. 10. Free boundary shapes for $\chi=0.2$ and $n=4$ are shown. (a) Closed equilibrium with $\gamma=1.6$, (b) $\gamma=2.22$, (c) $\gamma=2.22$, and (d) $\gamma=0.895$. [Note that (d) is a necked off equilibrium.]

$$h(r)\simeq n/(2r)^{(n-1)/n}. \tag{32}$$

At low pressure the free boundary is given in parametric form by

$$\frac{x}{a}=\frac{1}{2}\left(\frac{\gamma}{n}\right)^{1/(n-1)}\left(\cos(\omega)-\frac{\cos[(2n-1)\omega]}{2n-1}+\frac{2s\cos[(n-1)\omega]}{n-1}\right), \tag{33}$$

$$\frac{y}{a}=\frac{1}{2}\left(\frac{\gamma}{n}\right)^{1/(n-1)}\left(\sin(\omega)+\frac{\sin[(2n-1)\omega]}{2n-1}+\frac{2s\sin[(n-1)\omega]}{n-1}\right), \tag{34}$$

where

$$s\simeq-\chi r, \tag{35}$$

and where ω is in the range $0\leqslant\omega\leqslant\pi/2n$. Equations (33) and (34) can be used to find that the equilibria neck off unless s satisfies the inequality

$$|s|\leqslant\frac{(n-1)^2}{(2n-1)}\sin\left(\frac{\pi}{2(n-1)}\right). \tag{36}$$

The quantity α is given, in the low pressure limit, by

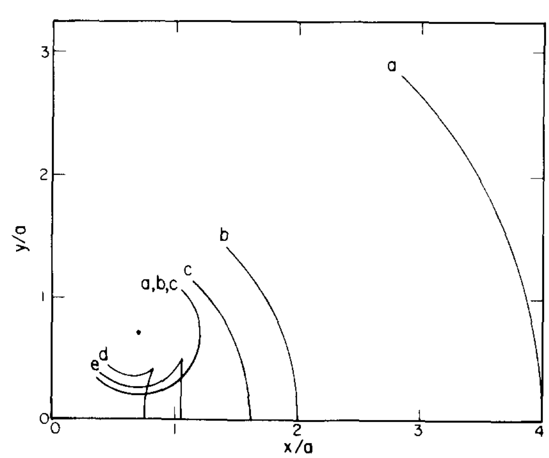

FIG. 11. Free boundary shapes for $\gamma=2$ and $n=4$ are shown. (a) Closed equilibrium with $\chi=1$, (b) closed equilibrium with $\chi=0$, (c) closed equilibrium with $\chi=-0.2$, (d) $\chi=0$, and (e) $\chi=-0.2$.

$$\alpha \simeq 1+\pi[(1-s^2)^{1/2}/s-\cos^{-1}(s)]^{-1}. \quad (37)$$

It is more convenient to describe low pressure cusp equilibria by n, a, b, I, and α, obtaining s from Eq. (37). For an octupole, the condition on s requires α to be in the range $1/10.85 \leq \alpha \leq 10.85$, so that the free boundary may have one segment quite elongated before necking off occurs.

For $n=2$ and for $\chi=0$, the free boundary shape equations should describe the quadrupole cusp obtained by Berkowitz *et al.*[7,8] in the low pressure limit. Indeed, if the z plane shown in Fig. 3 is rotated by 45°, then the parametric form for the free boundary shape in the rotated coordinates is

$$\frac{x'}{a}=\left(\frac{4\pi ab}{27\mu_0 I}\right)^{1/3}\cos^3\left(\omega-\frac{\pi}{4}\right), \quad (38)$$

$$\frac{y'}{a}=\left(\frac{4\pi ab}{27\mu_0 I}\right)^{1/3}\sin^3\left(\omega-\frac{\pi}{4}\right), \quad (39)$$

or, eliminating the parametric dependence,

$$\left(\frac{x'}{a}\right)^{2/3}+\left(\frac{y'}{a}\right)^{2/3}=\left(\frac{4\pi ab}{27\mu_0 I}\right)^{2/9}, \quad (40)$$

the familiar hypocycloid form. The coefficient on the right-hand side of Eq. (39) differs from that obtained by Berkowitz in that the quantity inside the parentheses is a factor of 2 bigger. The difference is understood by noting that in his quadrupole cusp there are four wires carrying current in alternating directions, while in the cusp considered here there are only two wires carrying current. Hence, his equivalent multipole at infinity is twice as strong for a given wire current as in the system considered here.

D. The high pressure limit

The high pressure limit corresponds to r near 1, as shown by Fig. 7. As $r\rightarrow 1$, the free boundary shape of the cusp equilibrium continuously approaches the two circular arcs of a closed equilibrium, although the approach is very slow, being characterized by the quantity $(r-1)^{1/4}$. In order to understand the nature of the bifurcation that occurs at high pressure, it is useful to examine the function $h(r)$ near $r=1$. Defining ϵ by

$$\epsilon = r-1 \quad (41)$$

and expanding the functions j and l defined in Eqs. (26) and (27) in ϵ yields, for the function h,

$$h(1+\epsilon)=(\chi+1-1/n)(n-\sqrt{\epsilon}\ln\epsilon)+O(\sqrt{\epsilon}). \quad (42)$$

If $\epsilon=0$, then $h=\gamma=n(\chi+1)-1$, the maximum value of γ for which a closed equilibrium exists. As ϵ increases from zero, the $O(\sqrt{\epsilon}\ln\epsilon)$ term dominates at first, causing h to increase; as ϵ increases further the $O(\sqrt{\epsilon})$ term dominates and h decreases, as shown in Fig. 7. Hence, for a range of γ slightly above $\gamma=n(\chi+1)-1$, there are two cusp equilibria for given values of n, a, I, and χ. For a range of γ below this value a closed equilibrium and a cusp equilibrium are obtained. [Recall that closed equilibria exist for γ in the range given in Eq. (7).] As γ is decreased further, the closed equilibria neck off; the cusp equilibria also neck off unless χ is near zero. For γ below $[\sin(\pi/n)]^{-1}$ and for χ near zero, one low pressure cusp equilibrium is obtained.

It is interesting to note that if we imagine a low pressure cusp equilibrium and imagine increasing the pressure, keeping the total flux fixed, i.e., holding I and χ constant, then there is no loss of equilibrium until γ exceeds the maximum value of $h(r)$; that is, the equilibria do not neck off under these conditions. This behavior is explained by noting that Eq. (31) requires $L_{DE}-L_{CD}$ to decrease as γ is increased, avoiding the elongation of one free boundary segment compared to the other that causes necking off. This indicates that for this highly idealized case, at least, it should be possible to "pump up" a multipole equilibrium from zero pressure to some maximum pressure in a flux conserving way.

IV. CONCLUSION

The hodograph method has been used to study bifurcation and the free boundary shapes in sharp boundary multipole equilibria and shows that two different equilibria may exist for given values of the external parameters. The particular form of the hodograph method used here is also well suited to the study of multipole systems enclosed in conducting walls as long as the wall cross section in the x-y plane is composed of straight line segments. With walls present, the images in the F and w planes become more complicated and elliptic functions are needed to effect the necessary mappings. Furthermore, in some cases the w plane image becomes multiply valued, making the mappings more difficult to carry out; the closed equilibria are also more difficult to calculate than the simple circular equilibria discussed in Sec. II. In spite of the difficulties, it would be interesting to study cusp equilibria in the presence of walls to see how the results obtained here are changed, and to look for bifurcation with a finite flux between the fluid and the wall held fixed.

Finally, in addition to whatever intrinsic interest there is in studying how different kinds of equilibria pass into one another, the results obtained here may be helpful in solving for diffuse magnetohydrodynamic equilibria in multipole geometries at high beta. Just as low pressure multipole equilibria have flux distributions resembling vacuum fields, high beta equilibria might be expected to resemble the equilibria calculated here. Thus, this calculation provides an upper end point in beta with which to compare diffuse equilibria. Also, since sharp boundary $\beta=1$ equilibria bifurcate, it might be expected that diffuse equilibria should also bifurcate for high beta and for narrow pressure profiles, i.e., the bifurcation between closed and cusp-like equilibria might have a diffuse boundary analog.

ACKNOWLEDGMENTS

The author thanks Dr. K. R. Symon and Dr. M. C. Shen for helpful suggestions and stimulating discussions.

This work was supported at the University of Wisconsin by the Department of Energy and the Danforth Foundation.

[1]J. M. Dawson, in *Proceedings of the Review Meeting on Advanced-Fuel Fusion* (Electric Power Research Institute, Palo Alto, Calif., 1977), p. 403.
[2]R. W. Conn, D. Arnush, J. Dawson, D. W. Kerst, and V. Vanek, in *Proceedings of the International Atomic Energy Agency Technical Committee Meeting and Workshop on Fusion Reactor Design Concepts*, Madison, Wisconsin, 1977 (International Atomic Energy Agency, Vienna, 1978), p. 721.
[3]M. W. Phillips, presented at the Sherwood Theoretical Meeting, Mount Pocono, Pennsylvania (1979).
[4]D. A. D'Ippolito, E. A. Adler, and Y. C. Lee, Phys. Fluids **23**, 794 (1980).
[5]H. Helmholtz, Philos. Mag. **36**, 337 (1868).
[6]L. M. Milne-Thomson, *Theoretical Hydrodynamics* (Macmillan, London, 1974), Chap. 12.
[7]J. Berkowitz, K. O. Friedrichs, H. Goertzel, H. Grad, J. Killeen, and E. Rubin, in *Proceedings of the Second United Nations International Conference on the Peaceful Uses of Atomic Energy* (United Nations, Geneva, 1958), Vol. 31, p. 171.
[8]J. Berkowitz, in *Proceedings of the Conference on Controlled Thermonuclear Reactions*, Gatlinburg, Tennessee, 1956 (Technical Information Service Extension, Oak Ridge, Tenn.), TID-7520, Pt. 2, p. 394.
[9]J. P. Freidberg and F. A. Haas, Phys. Fluids **16**, 1909 (1973).
[10]G. Becker, Nucl. Fusion **14**, 319 (1974).
[11]A. Kadish and D. C. Stevens, Nucl. Fusion **14**, 821 (1974).
[12]R. Gorenflo, Z. Angew. Math. Phys. **16**, 279 (1965).
[13]W. Kerner, D. Pfirsch, and H. Tasso, Nucl. Fusion **12**, 433 (1972).
[14]R. Gajewski, Phys. Fluids **15**, 70 (1972).
[15]H. R. Strauss, Phys. Fluids **17**, 1040 (1974).
[16]J. C. B. Papaloizou, I. Revelo, J. J. Field, C. L. Thomas, and F. A. Haas, Nucl. Fusion **17**, 33 (1977).
[17]B. D. Fried, J. W. Van Damm, and Y. C. Lee, Phys. Fluids **19**, 1909 (1976).
[18]J. A. Shercliff, J. Plasma Phys. **21**, 347 (1979).
[19]I. B. Bernstein, E. A. Frieman, M. D. Kruskal, and R. M. Kulsrud, Proc. Roy. Soc. London Ser. A **244**, 17 (1958).